Multicritical point of the three-dimensional $\mathbb{Z}_2$ gauge Higgs model

Claudio Bonati,[1] Andrea Pelissetto,[2] and Ettore Vicari[1]

[1]*Dipartimento di Fisica dell'Università di Pisa and INFN Largo Pontecorvo 3, I-56127 Pisa, Italy*
[2]*Dipartimento di Fisica dell'Università di Roma Sapienza and INFN Sezione di Roma I, I-00185 Roma, Italy*
(Dated: December 6, 2021)

We investigate the multicritical behavior of the three-dimensional $\mathbb{Z}_2$ gauge Higgs model, at the multicritical point (MCP) of its phase diagram, where one first-order transition line and two continuous Ising-like transition lines meet. The duality properties of the model determine some features of the multicritical behavior at the MCP located along the self-dual line. Moreover, we argue that the system develops a multicritical XY behavior at the MCP, which is controlled by the stable XY fixed point of the three-dimensional multicritical Landau-Ginzburg-Wilson field theory with two competing scalar fields associated with the continuous $\mathbb{Z}_2$ transition lines meeting at the MCP. This implies an effective enlargement of the symmetry of the multicritical modes at the MCP, to the continuous group O(2). We also provide some numerical results to support the multicritical XY scenario.

I. INTRODUCTION

The three-dimensional (3D) $\mathbb{Z}_2$ gauge Higgs model is one of the simplest gauge theories with matter fields, that shows a nontrivial phase diagram characterized by the presence of a topological phase, see, e.g., Refs. 1–19. The model can also be related to the quantum two-dimensional toric model in the presence of external *magnetic* fields, by a quantum-to-classical mapping[1,9,11], and to a statistical ensemble of membranes[7,12].

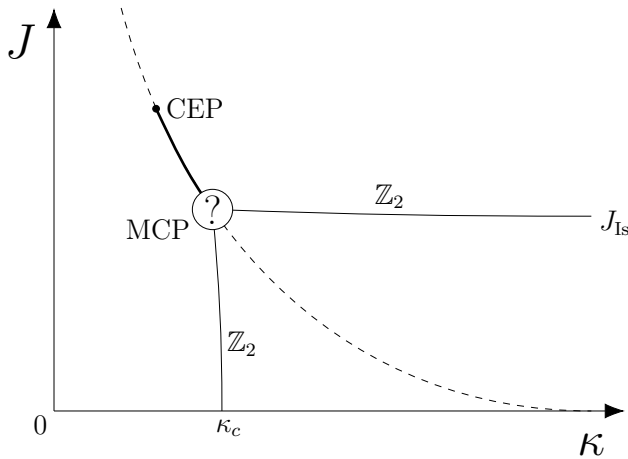A notable feature of the model[1,4,5] is the existence of a

FIG. 1: Sketch of the phase diagram of the 3D $\mathbb{Z}_2$ gauge Higgs model (1). The dashed line is the self-dual line, cf. Eq. (9), the thick line corresponds to first-order transitions on the self-dual line, extending for a finite interval. The two lines labelled "$\mathbb{Z}_2$" are related by duality, cf. Eq. (7), and correspond to Ising-like continuous transitions. They end at $J = J_{\mathrm{Is}} \approx 0.22165$, $\kappa = \infty$ and at $J = 0$, $\kappa = \kappa_c \approx 0.76141$. The three lines are conjectured to meet at a multicritical point (MCP) on the self-dual line, at $[\kappa^\star \approx 0.7525, J^\star \approx 0.2258]$. We argue in the paper that the multicritical behavior belongs to the XY universality class. The other endpoint of the first-order transition line should give rise to a critical endpoint (CEP).

duality transformation, which relates the free energy at different points of the phase diagram[1,3–5]. A particular line in the phase diagram, which will play an important role in the following, is the self-dual line which is left invariant by the duality transformation. In Fig. 1 we sketch the phase diagram of the model, in the space of the Hamiltonian parameters [they are defined in Eq. (1)]. It presents a topologically ordered deconfined phase, delimited by two continuous Ising transition lines that are related by duality. In the context of two-dimensional quantum systems, such a topological ordered phase is realized in $\mathbb{Z}_2$ spin liquids[20–25], which is the phase of matter realized by the toric code[9]. Moreover, the 3D $\mathbb{Z}_2$ gauge Higgs model presents a first-order transition line running along the self-dual line, for a limited range of the Hamiltonian parameters[6,8,11].

The available numerical results are consistent with the existence of a multicritical point (MCP), where the first-order transition line and the two continuous Ising transition lines meet, see, e.g., Refs. 11,17. Assuming the existence of the MCP, an interesting question concerns the nature of the multicritical behavior. This issue has been recently investigated in Ref. 17, which reported apparently puzzling results, leading to estimates of the critical exponents that are substantially consistent with those of the XY universality class. This may suggest that the multicritical behavior at the MCP is controlled by the 3D XY fixed point, with an effective enlargement of the symmetry of the multicritical modes to the continuous O(2) group. This scenario was considered unlikely in Ref. 17, because of the unclear relationship between the multicritical XY behavior and the mutual statistics of the condensing quasiparticles[10,11,26,27] along the two distinct Ising transition lines meeting at the MCP. These mutual statistics do not affect critical exponents on the Ising lines, because only one of the two excitations is massless on them, but both excitations must become massless at the MCP. Therefore, it is not clear how their competition can give rise to the effective enlargement of the symmetry at the MCP, as required by the XY universality class.

In this paper we investigate the multicritical behav-

ior at the MCP. We argue that the multicritical behavior is controlled by the stable XY fixed point of the 3D multicritical Landau-Ginzburg-Wilson (LGW) field theory with two competing scalar fields associated with the $\mathbb{Z}_2$ transition lines meeting at the MCP[28–32]. Duality properties play a crucial role for the realization of the multicritical XY scenario, which implies an effective enlargement of the symmetry of the multicritical modes, to the continuous symmetry group O(2). To provide further support to this scenario, we also report some numerical finite-size scaling (FSS) analyses of data from Monte Carlo (MC) simulations.

The paper is organized as follows. In Sec. II we present the 3D lattice $\mathbb{Z}_2$ gauge Higgs model, and summarize the known features of its phase diagram. In Sec. III we discuss the multicritical theory appropriate for the MCP, and apply the multicritical LGW field theory to predict a multicritical XY behavior. In Sec. IV we report some numerical results supporting the multicritical XY scenario, obtained by FSS analyses of MC simulations. Finally in Sec. V we draw our conclusions.

II. THE $\mathbb{Z}_2$ GAUGE HIGGS MODEL

A. Hamiltonian and duality transformations

We consider a lattice gauge model with $\mathbb{Z}_2$ gauge invariance defined on a cubic 3D lattice with periodic boundary conditions. The fundamental variables are Ising spins $s_{\boldsymbol{x}} = \pm 1$ defined on the lattice sites and Ising spins $\sigma_{\boldsymbol{x},\mu} = \pm 1$ defined on the bonds ($\sigma_{\boldsymbol{x},\mu}$ is associated with the bond starting from site $\boldsymbol{x}$ in the μ direction, $\mu = 1, 2, 3$). The model is defined by the lattice Hamiltonian[1,4,5]

$$H = -J \sum_{\boldsymbol{x},\mu} s_{\boldsymbol{x}}\, \sigma_{\boldsymbol{x},\mu}\, s_{\boldsymbol{x}+\hat{\mu}} - \kappa \sum_{\boldsymbol{x},\mu>\nu} \Pi_{\boldsymbol{x},\mu\nu}\,, \quad (1)$$

$$\Pi_{\boldsymbol{x},\mu\nu} = \sigma_{\boldsymbol{x},\mu}\, \sigma_{\boldsymbol{x}+\hat{\mu},\nu}\, \sigma_{\boldsymbol{x}+\hat{\nu},\mu}\, \sigma_{\boldsymbol{x},\nu}\,. \quad (2)$$

The corresponding partition function and free-energy density are

$$Z = \sum_{\{s,\sigma\}} e^{-\beta H(J,\kappa)}\,, \qquad F(J,\kappa) = -\frac{T}{L^d}\ln Z\,, \quad (3)$$

where $\beta = 1/T$ is the inverse temperature, and L^d is the volume of the system. This paper only consider three-dimensional systems, and therefore $d = 3$. However, when arguments are independent of the space dimension, we keep d generic. In the following, energies are measured in units of T, which is equivalent to fix $\beta = 1$ in Eq. (3).

The model can be simplified by considering the so-called unitary gauge. Indeed, the site variables $s_{\boldsymbol{x}}$ can be eliminated by redefining $\sigma_{\boldsymbol{x},\mu}$ as

$$s_{\boldsymbol{x}}\, \sigma_{\boldsymbol{x},\mu}\, s_{\boldsymbol{x}+\hat{\mu}}\ \to\ \sigma_{\boldsymbol{x},\mu}\,. \quad (4)$$

Correspondingly, the partition function can be written as

$$Z = \sum_{\{\sigma\}} e^{-H_{\mathrm{ug}}(J,\kappa)}\,, \quad (5)$$

$$H_{\mathrm{ug}} = -J \sum_{\boldsymbol{x},\mu} \sigma_{\boldsymbol{x},\mu} - \kappa \sum_{\boldsymbol{x},\mu>\nu} \Pi_{\boldsymbol{x},\mu\nu}\,. \quad (6)$$

An important property of the 3D lattice $\mathbb{Z}_2$ gauge Higgs model is the existence of a duality mapping[3] between the Hamiltonian parameters, that leaves the partition function unchanged, modulo a regular function of the parameters. If

$$(J',\kappa') = \left(-\frac{1}{2}\ln \tanh \kappa\,, -\frac{1}{2}\ln \tanh J \right)\,, \quad (7)$$

we have[3]

$$F(J',\kappa') = F(J,\kappa) - \frac{3}{2}\ln[\sinh(2J)\sinh(2\kappa)]\,. \quad (8)$$

One can also define a self-dual line,

$$D(J,\kappa) = J - J' = J + \frac{1}{2}\ln \tanh \kappa = 0\,, \quad (9)$$

where the duality transformation maps the model into itself, i.e. $J' = J$ and $\kappa' = \kappa$. Note that $D(J,\kappa)$ is odd under the duality mapping $(J,\kappa) \to (J',\kappa')$, i.e., $D(J,\kappa) = -D(J',\kappa')$.

B. The phase diagram

Some features of the phase diagram are well established, see, e.g., Refs. 4,11,17. A sketch of the phase diagram is shown in Fig. 1. For $\kappa \to \infty$ an Ising transition occurs at[33] $J_{\mathrm{Is}} = 0.221654626(5)$. By duality, in the pure $\mathbb{Z}_2$ gauge model a transition occurs in the corresponding point, $J = 0$ and

$$\kappa_c = -\frac{1}{2}\ln \tanh J_{\mathrm{Is}} = 0.761413292(11)\,. \quad (10)$$

Two Ising-like continuous transition lines, related by the duality transformation (7), start from these points[4] and intersect along the self-dual line[17]. Moreover, some numerical studies[8,11] have provided evidence of first-order transitions along the self-dual line, in the relatively small interval

$$0.688 \lesssim \kappa \lesssim 0.753\,, \qquad 0.258 \gtrsim J \gtrsim 0.226\,. \quad (11)$$

Since the first-order transition line is limited to an interval along the self-dual line, there are only two phases, separated by the two continuous transition lines, see Fig. 1. For small J and large κ there is a topological deconfined phase. The remaining part of the phase diagram corresponds to a single phase that extends from the disordered small-J,κ region to the whole large-J region. In particular, no phase transition occurs along the line $\kappa = 0$, where the model (6) becomes trivial.
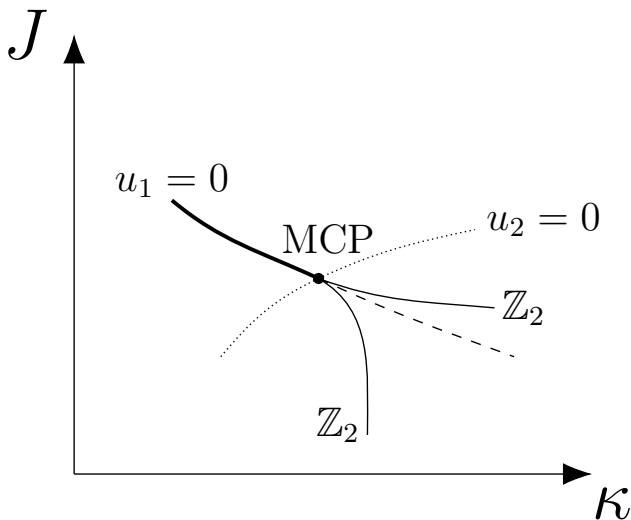
FIG. 2: Sketch of the phase diagram close to the MCP. We report the first-order transition line (thick line), the self-dual line (dashed line), the two continuous transition lines (continuous lines), and the line (dotted line) where $u_2 = 0$. The line $u_1 = 0$ coincides with the self-dual line.

A natural conjecture is that the first-order and the two continuous Ising transition lines meet at the same point located along the self-dual line, giving rise to a multicritical point (MCP). Numerical results[11,17] are consistent with this conjecture. In particular, Ref. 17 reported evidence of a critical transition point along the self-dual line—we identify it with the MCP—with critical parameters $\kappa^\star \approx 0.7526$ and $J^\star \approx 0.2257$. The corresponding critical exponents are close to, and substantially consistent with, those associated with the XY universality class[31,32,34,35]. In spite of these results, Ref. 17 considered an XY multicritical behavior unlikely. In the paper, we rediscuss the issue, and give additional theoretical and numerical arguments that support the hypothesis that the MCP belongs to the XY universality class.

We finally note that the first-order transition line starting from the MCP ends at $J \approx 0.258$ and $\kappa \approx 0.688$. We expect this endpoint to correspond to a continuous transition, likely belonging to the Ising universality class.

III. MULTICRITICAL BEHAVIOR

As discussed above, the phase diagram of the lattice $\mathbb{Z}_2$ gauge Higgs model shows a MCP, where a first-order and two continuous transition lines meet (this MCP is usually called bicritical[28–30]). In the following, we first discuss the expected behavior of the model close to the MCP, on the basis of the renormalization-group (RG) theory. Then, we discuss a a LGW field theory characterized by two interacting local real scalar fields[28–30,32], which may describe the multicritical behavior.

A. Multicritical scaling theory

At a MCP, the singular part of the free-energy density can be written as

$$F_{\text{sing}}(J, \kappa, L) = L^{-d}\mathcal{F}(\{u_i L^{y_i}\}), \qquad (12)$$

where u_i are the nonlinear scaling fields and the RG exponents y_i are ordered so that

$$y_1 > y_2 > y_3 > y_4 > ..., \qquad (13)$$

In the present model, we expect two relevant RG perturbations. Therefore, y_1 and y_2 are positive, and the corresponding scaling fields u_1 and u_2 vanish at the MCP. The exponents y_i with $i \geq 3$ are instead negative and control the corrections to the multicritical behavior. All the scaling fields u_i are analytic functions of the model parameters J and κ. In the infinite-volume limit and neglecting subleading corrections, we can rewrite the singular part of the free energy density as

$$F_{\text{sing}}(J, \kappa) = |u_2|^{d/y_2}\mathcal{F}_\pm(X), \qquad (14)$$

$$X \equiv u_1|u_2|^{-\phi}, \qquad \phi \equiv y_1/y_2 > 1, \qquad (15)$$

where the functions $\mathcal{F}_\pm(X)$ apply to the parameter regions in which $\pm u_2 > 0$, and ϕ is the so-called crossover exponent associated with the MCP. Close to the MCP, the transition lines follow the equation

$$X = u_1|u_2|^{-\phi} = \text{const}, \qquad (16)$$

with a different constant for each transition line. Since $\phi > 1$, they are tangent to the line $u_1 = 0$.

The duality mapping (7), and in particular Eq. (8), implies the relation

$$F_{\text{sing}}(J', \kappa') = F_{\text{sing}}(J, \kappa). \qquad (17)$$

Then, if we set

$$u_1' = u_1(J', \kappa'), \quad u_2' = u_2(J', \kappa'), \qquad (18)$$

using Eq. (14) we obtain the equality

$$|u_2|^{d/y_2}\mathcal{F}_\pm(u_1|u_2|^{-\phi}) = |u_2'|^{d/y_2}\mathcal{F}_\pm(u_1'|u_2'|^{-\phi}). \qquad (19)$$

Since along the self-dual line $u_1 = u_1' = 0$, this relation can only be satisfied if $|u_2| = |u_2'|$. If we then expand the scaling function $\mathcal{F}_\pm(X)$ in powers of X, Eq. (19) implies $u_1^m = (u_1')^m$ for all values of m such that the derivative

$$\mathcal{F}_m = \left.\frac{\partial^m \mathcal{F}(X)}{\partial X^m}\right|_{X=0} \qquad (20)$$

is nonvanishing. This condition can be satisfied only if u_1 changes at most by a sign under duality. As we shall argue below, u_1 is odd under duality, i.e., $u_1' = -u_1$. In this case, we should additionally require $\mathcal{F}_m = 0$ for any odd m: the functions $\mathcal{F}_\pm(X)$ are even in X.

To show that u_1 is odd, note that, as discussed in Sec. II B, the first-order transition line runs along the self-dual line (9) ending at the MCP, located at

$$J = J^\star, \quad \kappa = \kappa^\star = -\frac{1}{2}\ln\tanh J^\star. \quad (21)$$

This transition line is expected to coincide[28–30] with the line $u_1 = 0$, close to the MCP. Since the self-dual line is given by $D(J,\kappa) = 0$, we can make the identification

$$u_1 = D(J,\kappa), \quad (22)$$

close to the MCP. As noted before, $D(J,\kappa)$ is odd under duality. The scaling field u_2 is then necessarily even under duality and is therefore given by

$$u_2(J,k) = -J + J^\star + \frac{1}{2}\ln\frac{\tanh\kappa}{\tanh\kappa^\star}. \quad (23)$$

The scaling fields can be straightforwardly linearized obtaining

$$u_1 \approx \Delta J + c\,\Delta\kappa, \qquad u_2 \approx -\Delta J + c\,\Delta\kappa, \quad (24)$$

where

$$\Delta J = J - J^\star, \qquad \Delta\kappa = \kappa - \kappa^\star,$$
$$c = \sinh(2J^\star) = \frac{1}{\sinh(2\kappa^\star)} \approx 0.467. \quad (25)$$

In terms of u_1 and u_2, close to the MCP the first-order transition line corresponds to $X = 0$, $u_2 < 0$. The two continuous transition lines are defined by $X = \pm k$ with $u_2 > 0$.

Using the above results we can also predict how the latent heat Δ_h vanishes along the first-order transition line when approaching the MCP. A straightforward scaling argument[36] gives

$$\Delta_t \sim |u_2|^\theta, \qquad \theta = \frac{d - y_1}{y_2}. \quad (26)$$

Note that this scaling behavior is the same as that of the magnetization M at the Ising transition, with the correspondence $y_1 = y_h$ and $y_2 = 1/\nu$: M indeed vanishes as $M \sim |T - T_c|^\beta$ with $\beta = (d - y_h)\nu$, see, e.g., Ref. 31.

B. Scaling of the energy cumulants

Due to the fact that we are considering a lattice gauge theory, and therefore that we cannot easily access the order parameters associated with the phase transitions, we focus on the multicritical behavior of the energy operators. We define

$$H_J = \sum_{x\,\mu}\sigma_{x,\mu}, \qquad H_\kappa = \sum_{x\,\mu>\nu}\Pi_{x,\mu\nu}, \quad (27)$$
$$H = -JH_J - \kappa H_\kappa.$$

We consider the cumulants

$$C_{nm} = -L^d\frac{\partial^{n+m}}{\partial J^n\partial\kappa^m}F(J,\kappa,L), \quad (28)$$

where F is the free-energy density. For $n+m \leq 3$, $C_{nm} = M_{nm}$, where M_{nm} are the central moments defined by

$$M_{nm} = \langle(H_J - E_J)^n(H_\kappa - E_\kappa)^m\rangle, \quad (29)$$

with $E_J = \langle H_J\rangle$ and $E_\kappa = \langle H_\kappa\rangle$. For $n + m \geq 4$, central moments and cumulants differ. For instance, $C_{40} = M_{40} - 3M_{20}^2$.

Using the cumulants C_{mn} we can easily construct the cumulants K_n of the total energy H, defined by the derivatives of $\ln Z$ with respect to β, see Eq. (3). For example, we have

$$K_2 = J^2C_{20} + 2J\kappa C_{11} + \kappa^2C_{02}, \quad (30)$$
$$K_3 = -\left(J^3C_{30} + 3J^2\kappa C_{21} + 3J\kappa^2C_{12} + \kappa^3C_{03}\right),$$

etc... Note that the specific heat is given by $C_V = K_2/V$.

In the following, we consider periodic boundary conditions, which preserve the duality property in finite-size systems. Using Eq. (8), and taking the appropriate derivatives with respect to J and κ, we can obtain an infinite series of exact relations among the expectation values E_J, E_κ and the cumulants C_{mn} at (J,κ) and at the corresponding duality-transformed couplings (J',κ'), cf. Eq. (7). Along the self-dual line where $(J,\kappa) = (J',\kappa')$, they turn into an infinite series of exact relations among expectation values of cumulants computed on the self-dual line. The lowest-order cumulants satisfy the relations

$$E_\kappa + \sinh(2J)\,E_J - 3\cosh(2J)L^3 = 0, \quad (31)$$
$$\sinh^2(2J)\,C_{20} - C_{02} - 2\cosh(2J)\,E_\kappa + 6L^3 = 0. \quad (32)$$

Relations for higher-order cumulants are more cumbersome. Neglecting the regular terms arising from the second term of the r.h.s. of Eq. (7), third-order cumulants satisfy the relations

$$C_{12} + \sinh(2J)\,C_{21} + 2\cosh(2J)\,C_{11} \approx 0, \quad (33)$$
$$C_{03} + \sinh^3(2J)\,C_{30} + 6\cosh(2J)\,C_{02} +$$
$$+2[3 + \cosh(4J)]E_\kappa \approx 0.$$

The scaling behavior of the cumulants C_{nm} can be derived by differentiating the asymptotic scaling relation

$$F_{\text{sing}}(J,\kappa,L) \approx L^{-d}f(x_1,x_2), \qquad x_i = u_iL^{y_i}, \quad (34)$$

where we only keep the relevant RG contributions. Note that the duality relation (8) for the free energy, and the duality properties of u_1 and u_2, imply that

$$f(-x_1,x_2) = f(x_1,x_2). \quad (35)$$

Introducing the derivatives

$$f_{n,m}(x_1,x_2) = \frac{\partial^{n+m}f(x_1,x_2)}{\partial x_1^n\partial x_2^m}, \quad (36)$$

the leading critical contribution is generally given by

$$C_{nm}(J, \kappa, L) \approx u_{1,J}^n u_{1,\kappa}^m L^{(n+m)y_1} f_{n+m,0}(x_1, x_2) , \quad (37)$$

where $u_{1,J}$ and $u_{1,\kappa}$ are the derivatives of u_1 with respect to J and κ. The cumulants of the total energy are expected to develop an analogous scaling behavior, i.e.

$$K_n(J, \kappa, L) \approx L^{ny_1} \mathcal{K}_n(x_1, x_2) . \quad (38)$$

Along the self-dual line $u_1 = 0$ the duality symmetry leads to some cancellations, as a consequence of Eq. (35). For $n + m$ even, the leading terms of the cumulants C_{nm} are given by

$$\begin{aligned} C_{nm}(J, \kappa, L) &\approx u_{1,J}^n u_{1,\kappa}^m L^{(n+m)y_1} f_{n+m,0}(0, x_2) \\ &\approx c^m L^{(n+m)y_1} f_{n+m,0}(0, x_2) . \end{aligned} \quad (39)$$

Note that Eq. (39) is consistent with the exact relations derived from duality, such as Eq. (32). For $n + m$ odd, the relation (35) implies that

$$f_{n+m,0}(0, x_2) = 0 . \quad (40)$$

Therefore, the leading scaling behavior is obtained by differentiating once with respect to u_2. Thus, for odd $n + m$ we obtain

$$\begin{aligned} C_{nm} &\approx L^{(n+m-1)y_1+y_2} f_{n+m-1,1}(0, x_2) \times \quad (41) \\ &\quad \times (n \, u_{1,J}^{n-1} u_{1,\kappa}^m u_{2,J} + m \, u_{1,J}^n u_{1,\kappa}^{m-1} u_{2,\kappa}) \\ &\approx (m - n) c^m L^{(n+m-1)y_1+y_2} f_{n+m-1,1}(0, x_2) , \end{aligned}$$

where $u_{2,J}$ and $u_{2,\kappa}$ are the derivatives of u_2 with respect to J and κ, respectively. Using these asymptotic behaviors along the self-dual line and the relations (30), we can also derive the corresponding asymptotic FSS of the cumulants K_n of the total energy, which behave as

$$K_n \approx L^{ny_1} \widetilde{\mathcal{K}}_n(x_2) \quad \text{for even } n , \quad (42)$$
$$K_n \approx L^{(n-1)y_1+y_2} \widetilde{\mathcal{K}}_n(x_2) \quad \text{for odd } n . \quad (43)$$

It is also useful to consider combinations whose cumulants have definite properties under duality transformations. We define

$$A = H_J - \sinh(2\kappa) H_\kappa , \quad (44)$$
$$S = H_J + \sinh(2\kappa) H_\kappa . \quad (45)$$

Since

$$\frac{\partial u_1}{\partial J} + \sinh(2\kappa) \frac{\partial u_1}{\partial \kappa} = 0 , \quad (46)$$
$$\frac{\partial u_2}{\partial J} - \sinh(2\kappa) \frac{\partial u_2}{\partial \kappa} = 0 ,$$

one can easily check that the cumulants A_n of the operator A, defined in Eq. (44), do not receive contributions associated with the scaling field u_1. Therefore, they generally scale as

$$A_n \approx L^{ny_2} \mathcal{A}_n(x_1, x_2) , \quad \mathcal{A}_n = (-2)^n f_{0n}(x_1, x_2) . \quad (47)$$

The cumulants S_n of the operator S behave as

$$S_n \approx L^{ny_1} \mathcal{S}_n(x_1, x_2) , \quad \mathcal{S}_n = 2^n f_{n0}(x_1, x_2) . \quad (48)$$

Along the self-dual line, however, this diverging behavior is not observed for n odd, since $f_{n0}(0, x_2) = 0$, thus S_n is expected to diverge as $L^{(n-1)y_1}$.

We finally note that the above scaling equations assume that the leading contribution is due to the singular part of the free energy. However, contributions due to the regular free-energy term, of order L^d, may provide the leading contribution for the lowest-order cumulants, depending on the values of the RG exponents y_1 and y_2.

C. Multicritical field theory

The results of Sections III A and III B only rely on the existence of a duality transformation and make no assumption on the nature of the MCP. To go further and make more quantitative predictions, it is crucial to understand the nature of the order parameters. Along the finite-J transition line that ends at $\kappa = \infty$, the order parameter is expected to be a local function of the s_x fields, which should correspond to the Ising magnetization. Of course, because of gauge invariance, any rigorous definition requires the introduction of an appropriate gauge fixing, which however would not change any gauge-invariant correlation function (in Ref. 37 this approach has been used to obtain rigorous results for the phase behavior of the U(1) Abelian-Higgs model). The order parameter for the $\mathbb{Z}_2$ gauge theory is instead expected to be nonlocal and indeed the transition has a topological nature. Apparently, this observation seems to indicate that one cannot use standard symmetry arguments to understand the critical behavior at the MCP, as they assume that the order parameters are coarse-grained local functions of the microscopic fields.

We wish now to argue that, at the MCP (and only there), because of duality, we can assume that both order parameters are local. Strictly speaking, duality is only a mapping of the Hamiltonian parameters, but here we will enlarge its role and assume that duality provides a mapping for all RG operators. Essentially, let us assume that we are working in the infinite-dimensional space of Hamiltonians on which the RG transformations act[38]. If we start from a $\mathbb{Z}_2$ gauge Hamiltonian, under RG transformations, we will generate a flow towards a $\mathbb{Z}_2$ gauge-invariant fixed point, while starting from the usual Ising model, we will observe a flow towards the Wilson-Fisher $\mathbb{Z}_2$ fixed point. The existence of an exact microscopic relation between the $\mathbb{Z}_2$ gauge model and the Ising model allows us to conjecture that the two fixed points are equivalent, with the same set of RG dimensions and operators. In other words, there is a mapping (we call it duality) between all RG operators at the different fixed points. It is then plausible that this duality transformation maps the local order parameter of the Ising model to the nonlocal order parameter of the gauge model. The

mapping changes the Hamiltonian parameters, except on the self-dual line, and therefore at the MCP. Here, the mapping would imply the equivalence of the local and of the nonlocal order parameters for the same model. Therefore, it seems reasonable to describe the multicritical behavior in terms of two local quantities. We thus consider two different scalar fields $\varphi_1(\boldsymbol{x})$ and $\varphi_2(\boldsymbol{x})$, associated with the two transition lines.

To derive a Lagrangian for the effective model, we note that the theory should be invariant under a change of sign of both fields, so that only even powers of each field are allowed. Under these conditions the LGW Hamiltonian is[28–30]

$$\mathcal{H} = \frac{1}{2}\Big[(\partial_\mu\varphi_1)^2 + (\partial_\mu\varphi_2)^2\Big] + \frac{1}{2}\Big(r_1\varphi_1^2 + r_2\varphi_2^2\Big) + \frac{1}{4!}\Big[v_1\varphi_1^4 + v_2\varphi_2^4 + 2w\,\varphi_1^2\varphi_2^2\Big]. \quad (49)$$

This model has been studied at length. In the mean-field approximation[28–30], the field theory (49) admits a bicritical point analogous to the one appearing in Fig. 2. Moreover, if the transition is continuous, it should belong to the XY universality class[28–32] thereby leading to an effective enlargement of the symmetry from $\mathbb{Z}_2 \oplus \mathbb{Z}_2$ to $O(2)$.

Several field-theoretical and numerical works have determined the exponents y_i entering the multicritical scaling ansatz (12), see, e.g., Refs. 32,35. As shown in Ref. 32, the leading exponents correspond to the RG dimensions at the isotropic XY fixed point of quadratic and quartic perturbations that belong to different representations of $O(2)$ group. The leading RG exponent y_1 is associated with the quadratic spin-two perturbation. The corresponding RG dimension is[32,35]

$$y_1 = 1.7639(11). \quad (50)$$

The second largest exponent is associated with the spin-zero quadratic operator, and is directly related to the correlation-length critical exponent at standard XY transitions:

$$y_2 = \frac{1}{\nu_{xy}} = 1.4888(2), \quad (51)$$

where we used the estimate $\nu_{xy} = 0.6717(1)$ (see, e.g., Refs. 31,34,39–42 for theoretical results by various methods). Using the above results, we can estimate the crossover exponent,

$$\phi = y_1/y_2 = 1.1848(8). \quad (52)$$

Scaling corrections at the multicritical XY point are controlled by the negative RG dimensions y_i. The most relevant ones are[32,35,41,43]

$$y_3 = -0.108(6), \quad (53)$$
$$y_4 = -0.624(10), \quad (54)$$
$$y_5 = -0.789(4), \quad (55)$$

which are related to the spin-4, spin-2, and spin-zero quartic perturbations, respectively. Note that, at standard XY transitions, corrections decay as $L^{-\omega}$ with $\omega = -y_5 \approx 0.79$. At the MCP, scaling corrections decay much slower, as $L^{y_3} \approx L^{-0.108}$, which may complicate the analysis of the universal multicritical XY behavior. Moreover, corrections with any integer combination of the subleading exponents are also expected, and thus corrections L^{ny_3} with $n = 2, 3, \ldots$ should also appear.

In the LGW approach the analogue of the duality mapping is the exchange of the two fields ($\varphi_1 \to \varphi_2$, $\varphi_2 \to \varphi_1$). The RG operators associated with the scaling fields u_i must have definite properties under these transformations. The leading operator of RG dimension y_1 is odd under the field exchange. This implies that u_1 is odd under the simultaneous exchange of r_1, r_2 and of v_1, v_2. In the $\mathbb{Z}_2$ gauge Higgs model this implies that the scaling field u_1 is odd under duality, in agreement with the arguments presented in Sec. III A. Analogously, we predict u_2 to be even, as already discussed before. We can also predict the transformation properties of the irrelevant scaling fields: u_3 and u_5 are even functions under duality, while u_4 is odd. In particular, there are no corrections with exponent y_4 on the self-dual line.

IV. NUMERICAL RESULTS

In this section we report some numerical results supporting our hypothesis of an emerging XY multicriticality at the MCP, as discussed in the previous sections. For this purpose, we present FSS analyses of MC simulations of the unitary-gauge model (6), using a standard Metropolis upgrading of the discrete spin link variables[44]. We consider cubic systems of size L with periodic boundary conditions.

We perform simulations along the self-dual line $u_1 = 0$ and along the line $u_2 = 0$, measuring the energy cumulants defined in Sec. III B. We verify the predicted FSS behavior, using the RG exponents $y_1 = 1.7639(11)$ and $y_2 = 1.4888(2)$ of the XY universality class. We should remark that the observation of the asymptotic scaling behaviors predicted by the multicritical XY scenario is made difficult by the existence of several sources of slowly decaying scaling corrections. The leading ones decay very slowly, as $L^{ny_3} \approx L^{-0.108n}$ with $n = 1, 2, \ldots$. Then, we should consider terms decaying as $L^{-(y_1-y_2)} \approx L^{-0.28}$ [they are absent on the self-dual line because of Eq. (35)], as $L^{-2(y_1-y_2)} \approx L^{-0.55}$, $L^{-y_4} \approx L^{-0.62}$ (they are absent along the self-dual line), $L^{-y_5} \approx L^{-0.79}$. For $m + n = 2$ also the regular background plays a role, giving rise to corrections of order $L^{3-2y_1} \approx L^{-0.53}$.

Along the self-dual line the scaling field u_1 vanishes. Thus, according to the RG analysis reported in Sec. III B, we expect that the asymptotic scaling behavior of the energy cumulants depends on the FSS variable $x_2 = u_2 L^{y_2}$. Along the self-dual line the numerical FSS analyses of the energy cumulants K_n, A_n, S_n are consistent with the
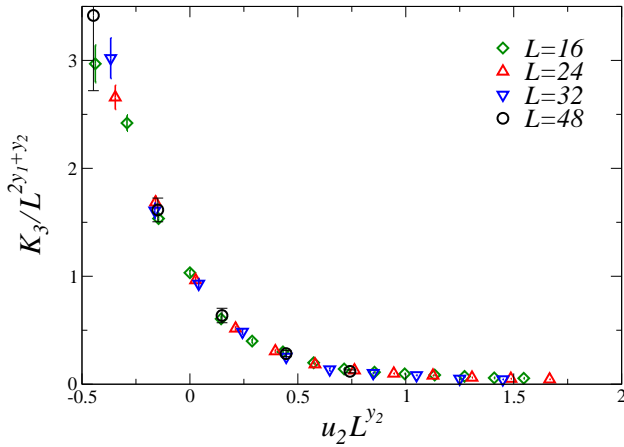
FIG. 3: Scaling behavior of the third cumulant K_3 of the Hamiltonian along the $u_1 = 0$ line as a function of $u_2 L^{y_2}$. We use the XY exponents $y_1 = 1.7639$, $y_2 = 1.4888$ and $\kappa^\star = 0.7525$.

predictions of the multicritical theory, see Eqs. (42) and (43) for the total energy, once the XY values of the RG exponents reported in Eqs. (50) and (51) are used. The most accurate estimate of the MCP point is obtained by biased analyses of the third cumulant $A_3 \sim L^{3y_2}$ of the operator A, see Eq. (44), along the self-dual line, using the XY values for the exponents. Fitting the data to Eq. (47), we obtain

$$\kappa^\star = 0.7525(1), \quad J^\star = 0.22578(5). \quad (56)$$

This estimate of the MCP is consistent with the results reported in Ref. 17. The analysis of the other cumulants gives consistent results.

The accuracy of the description in terms of the multicritical XY predictions is demonstrated by the scaling plots of the data of the cumulants using the XY exponents and the estimates (56). In Fig. 3 we show data for the third cumulant K_3 of the Hamiltonian, which is expected to scale with the power law $L^{2y_1+y_2}$, cf. Eq. (43). We observe a reasonably good scaling: scaling corrections are hardly visible within the statistical errors. Note that, according to the multicritical XY scenario, one expects slowly decaying corrections with exponent $|y_3| \approx 0.11$, cf. Eq. (53). We do not observe them here. In our range of values of L, L^{y_3} varies only slightly, and thus it is conceivable that they do not affect the divergent behavior of the observables, but only the accuracy of the scaling functions. In Fig. 4 we report the scaling plots of A_3 and A_4. Data are again in good agreement with the theoretical predictions for their asymptotic scaling behavior, cf. Eqs. (47). We do not report the second cumulant A_2, whose singular part should scale as L^{2y_2}. Since $2y_2 \approx 2.9775 < 3$, its behavior is dominated by the regular contribution, that scales as the volume L^3.

Beside checking the consistency of the numerical data with the multicritical XY scenario, we can also perform unbiased fits, to determine y_1 and y_2. If we fit the third
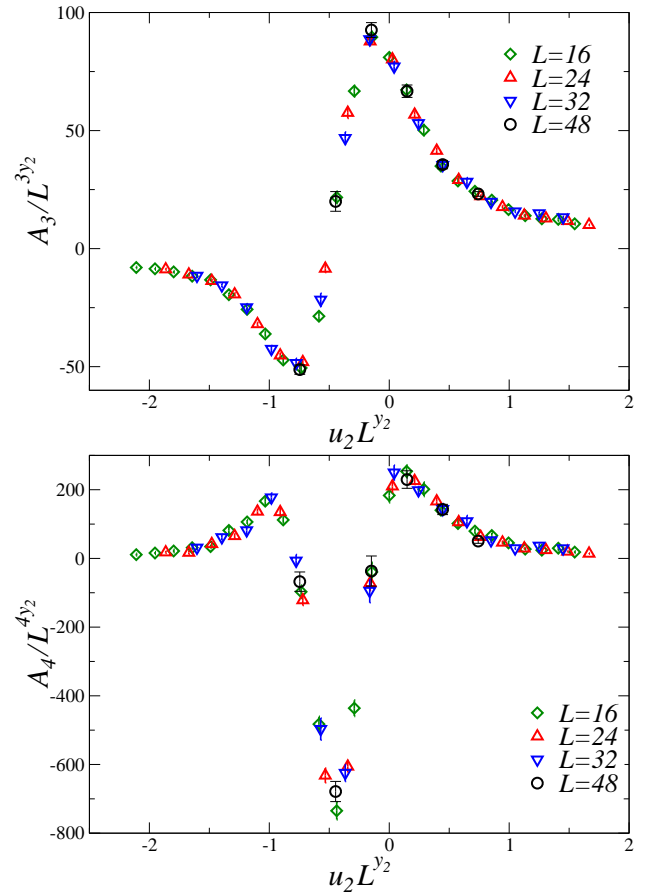

FIG. 4: Scaling behavior of cumulants A_3 (top) and A_4 (bottom) along the $u_1 = 0$ line as a function of $u_2 L^{y_2}$. We use the XY exponents $y_1 = 1.7639$, $y_2 = 1.4888$ and $\kappa^\star = 0.7525$.

and fourth cumulant of the Hamiltonian (they should scale as $K_3 \sim L^{2y_1+y_2}$ and $K_4 \sim L^{4y_1}$, respectively) we obtain $2y_1 + y_2 = 5.0(1)$ and $4y_1 = 7.0(1)$, which are consistent with the predictions $2y_1 + y_2 \approx 5.02$ and $4y_1 \approx 7.06$. The exponent y_2 can also be estimated from A_n. We obtain $y_2 = 1.495(10)$ and $y_2 = 1.48(2)$ from A_3 and A_4, respectively. The agreement with the conjectured XY values is quite good.

We also performed simulations along the $u_2 = 0$ line, see Eq. (23), using the estimate $\kappa^\star = 0.7525$ obtained from the FSS analyses along the self-dual $u_1 = 0$ line. Along the $u_2 = 0$ line, the asymptotic FSS of the cumulants of the total energy is that given in Eq. (38), i.e.

$$K_n \approx L^{ny_1} \mathcal{K}_n(x_1, 0). \quad (57)$$

Note that, for n odd, consistency with the FSS behavior along the self-dual line, see Eq. (43), requires $\mathcal{K}_n(0,0) = 0$. The data are plotted in Fig. 5, We observe a nice collapse of the data, again fully supporting the multicritical XY scenario.

Finally, we also check the scaling behavior of the third cumulants of A and S along the $u_2 = 0$ line, in Fig. 6. The scaling behavior of the cumulants of A is given in
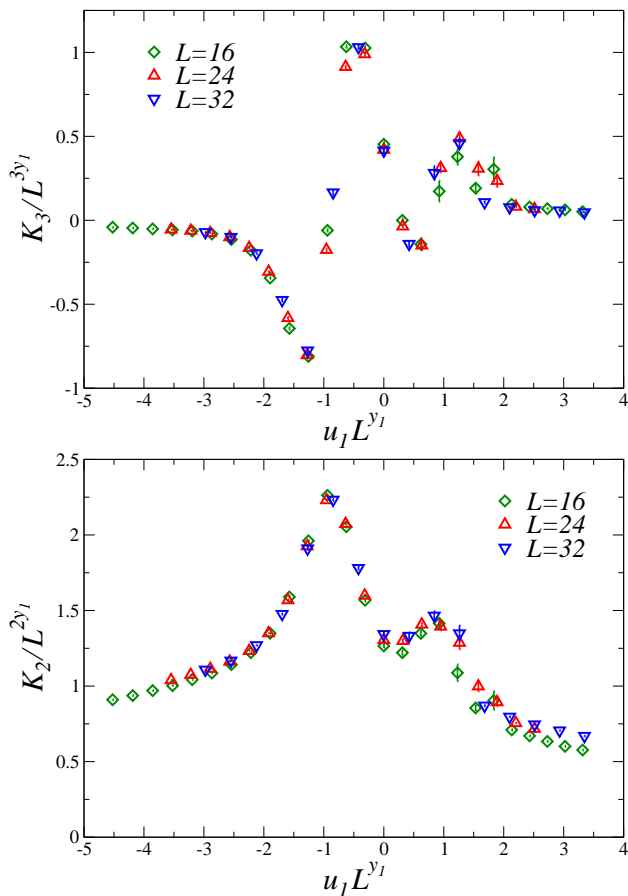
FIG. 5: Scaling plot of the second cumulant K_2 (bottom) and of the third cumulant K_3 (top) of the Hamiltonian along the $u_2 = 0$ line, using the XY exponent $y_1 = 1.7639$ and $\kappa^\star = 0.7525$. Data confirm the scaling prediction, Eq. (57) . Notice that the error bars of K_3 for $u_1 L^{y_1} \gtrsim 1$ may be underestimated. In this region of the phase diagram we observe an increasing inefficiency of the MC algorithm.
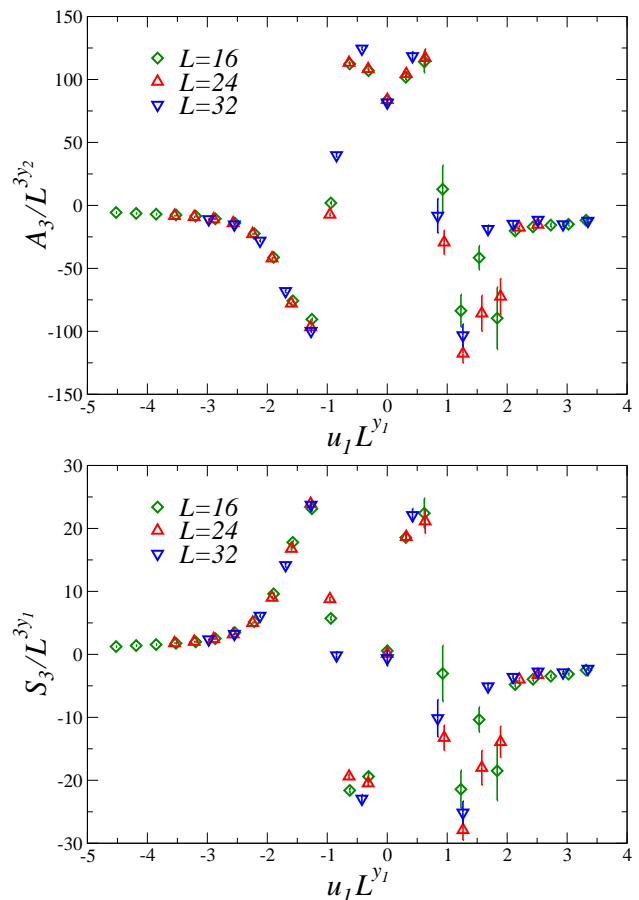
FIG. 6: Scaling plot of the third cumulants A_3 (top) and S_3 (bottom) of the operators A and S along the $u_2 = 0$ line, using the XY exponents $y_1 = 1.7639$ and $y_2 = 1.4888$, and $\kappa^\star = 0.7525$.

Eq. (47). It depends on $f_{0n}(x_1, 0)$ which is always an even function of x_1. The data shown in the top Fig. 6 are definitely consistent within the errors. As for the cumulants of S, they scale as reported in Eq. (48). Relation (35) implies that the odd (resp. even) cumulants are odd (resp. even) functions of x_1. Again, this is confirmed by the data shown in the bottom Fig. 6. In particular, the ratio S_3/L^{3y_1} is consistent with zero at the critical point $x_1 = 0$.

Note that statistical errors of the MC simulations along $u_2 = 0$ line increase significantly in the region $x_1 \gtrsim 1$. The link update algorithm for the model (6) becomes indeed less efficient as κ and J are increased. Autocorrelation times increase by more than one order of magnitude, likely due to a different dynamic regime related to the presence of relevant nonlocal configurations, which are hardly modified by local moves.

The results we have presented here complement those reported in Ref. 17, which were already providing a remarkable evidence of the multicritical XY behavior (al-

though the authors were quite skeptical on its interpretation in terms of a multicritical XY behavior). In particular, their estimates of the multicritical exponents $y_1 = 1.778(6)$ and $y_2 = 1.495(9)$ (other compatible, but less precise, results were also reported in Refs. 10,13) are in substantial agreement with the XY predictions (50) and (51). The small difference in the estimate of y_1 can be easily explained by the very slowly decaying scaling corrections predicted by the multicritical XY scenario, that make a precise determination of the universal asymptotic quantities very hard. The leading one vanishes as $L^{-0.108}$, so that, to reduce it by a factor of two, the lattice size must be increased by a factor of 600, which is unattainable in practice.

Overall, we believe that the numerical results presented in this paper, and those already reported in Ref. 17, provide strong evidence of the multicritical XY scenario put forward in the previous sections.

V. CONCLUSIONS

We study the multicritical behavior of 3D $\mathbb{Z}_2$ gauge Higgs model at the MCP, where one first-order transition line and two continuous Ising transition lines meet, as sketched in Fig. 1. The duality properties of the model play a key role in the phase diagram, and in determining the main features of the multicritical behavior at the MCP located on the self-dual line.

We exploit duality to identify the scaling fields associated with the relevant RG perturbations at the MCP, and outline the corresponding multicritical scaling behaviors. Moreover, we present arguments supporting the identification of the multicritical universality class with the one controlled by the stable XY fixed point of the 3D multicritical LGW field theory (49), with two competing

scalar fields associated with the continuous $\mathbb{Z}_2$ transition lines meeting at the MCP. The XY nature of the MCP implies an effective enlargement of the symmetry of the multicritical modes, to the continuous group O(2).

We have also reported numerical FSS analyses of several energy cumulants. The results are in good agreement with the theoretical predictions based on the multicritical XY scenario. We believe that our numerical results, together with those already reported in the literature, see, in particular, Ref. 17, provide a strong evidence in favor of the multicritical XY scenario at the MCP. Of course, this picture calls for a deeper understanding of the mechanisms that combine the local and nonlocal critical modes of the $\mathbb{Z}_2$ gauge Higgs model to give rise to the multicritical XY behavior, entailing an effective enlargement of the symmetry at the MCP, to the continuous group O(2).

[1] F. J. Wegner, Duality in generalized ising models and phase transitions without local order parameters, Jour. of Math. Phys. **12**, 2259 (1971).

[2] R. Balian, J. M. Drouffe, and C. Itzykson, Gauge fields on a lattice. i. general outlook, Phys. Rev. D **10**, 3376 (1974).

[3] R. Balian, J. M. Drouffe, and C. Itzykson, Gauge fields on a lattice. II. Gauge-invariant Ising model, Phys. Rev. D **11**, 2098 (1975).

[4] E. Fradkin and S. Shenker, Phase diagrams of lattice gauge theories with Higgs fields, Phys. Rev. D **19**, 3682 (1979).

[5] J. B. Kogut, An introduction to lattice gauge theory and spin systems, Rev. Mod. Phys. **51**, 659 (1979).

[6] G. A. Jongeward, J. D. Stack, and C. Jayaprakash, Monte carlo calculations on Z_2 gauge-higgs theories, Phys. Rev. D **21**, 3360 (1980).

[7] D. A. Huse and St. Leibler, Are sponge phases of membranes experimental gauge-higgs systems?, Phys. Rev. Lett. **66**, 437 (1991).

[8] L. Genovese, F. Gliozzi, A. Rago, and C. Torrero, The phase diagram of the three-dimensional Z_2 gauge Higgs system at zero and finite temperature, Nucl. Phys. B Proc. Suppl. **119**, 894 (2003).

[9] A. Kitaev, Fault-tolerant quantum computation by anyons, Ann. Phys. New York **303**, 2 (2003).

[10] J. Vidal, S. Dusuel, and K. P. Schmidt, Low-energy effective theory of the toric code model in a parallel magnetic field, Phys. Rev. B **79**, 033109 (2009).

[11] I. S. Tupitsyn, A. Kitaev, N. V. Prokofev, and P. C. E. Stamp, Topological multicritical point in the phase diagram of the toric code model and three-dimensional lattice gauge Higgs model, Phys. Rev. B **82**, 085114 (2010).

[12] K. Gregor, D. A. Huse, R. Moessner, and S. L. Sondhi, Diagnosing deconfinement and topological order, New Jour. of Phys. **13**, 025009 (2011)

[13] S. Dusuel, M. Kamfor, R. Orus, K. P. Schmidt, and J. Vidal, Robustness of a perturbed topological phase, Phys. Rev. Lett. **106**, 107203 (2011).

[14] F. Wu, Y. Deng, and N. Prokofev, Phase diagram of the toric code model in a parallel magnetic field, Phys. Rev. B **85**, 195104 (2012).

[15] E. Fradkin, *Field theories of condensed matter physics* (Cambridge University Press, 2013).

[16] S. Sachdev, Topological order, emergent gauge fields, and Fermi surface reconstruction, Rep. Prog. Phys. **82**, 014001 (2019).

[17] A. Somoza, P. Serna, and A. Nahum, Self-dual criticality in three-dimensional $\mathbb{Z}_2$ gauge theory with matter, Phys. Rev. X **11**, 041008 (2021).

[18] M. Grady, Exploring the 3D Ising gauge-Higgs model in exact Coulomb gauge and with a gauge-invariant substitute for Landau gauge, arXiv:2109.04560.

[19] L. Homeier, C. Schweizer, M. Aidelsburger, A. Fedorov, and F. Grusdt, $\mathbb{Z}_2$ lattice gauge theories and Kitaev's toric code: A scheme for analog quantum simulation, arXiv:2012.05235.

[20] N. Read and B. Chakraborty, Statistics of the excitations of the resonating-valence-bond state, Phys. Rev. B **40**, 7133 (1989).

[21] S. Kivelson, Statistics of holons in the quantum hard-core dimer gas, Phys. Rev. B **39**, 259 (1989).

[22] N. Read and S. Sachdev, Large-n expansion for frustrated quantum antiferromagnets, Phys. Rev. Lett. **66**, 1773 (1991).

[23] X.-G. Wen, Mean-field theory of spin-liquid states with finite energy gap and topological orders, Phys. Rev. B **44**, 2664 (1991).

[24] T. Senthil and M. P. A. Fisher, Z_2 gauge theory of electron fractionalization in strongly correlated systems, Phys. Rev. B **62**, 7850 (2000).

[25] R. Moessner, S. L. Sondhi, and E. Fradkin, Short-ranged resonating valence bond physics, quantum dimer models, and ising gauge theories, Phys. Rev. B **65**, 024504 (2001).

[26] S. D. Geraedts and O. I. Motrunich, Monte Carlo study of a U(1)⊗U(1) system with π-statistical interaction, Phys. Rev. B **85**, 045114 (2012).

[27] F. J. Burnell, Anyon condensation and its applications, Ann. Rev. Cond. Matt. Phys. **9**, 307 (2018).

[28] K.-S. Liu and M. E. Fisher, Quantum lattice gas and the existence of a supersolid, J. Low Temp. Phys. **10**, 655 (1972).

[29] M. E. Fisher and D. R. Nelson, Spin Flop, Supersolids, and Bicritical and Tetracritical Points, Phys. Rev. Lett. **32**, 1350 (1974).

[30] D. R. Nelson, J. M. Kosterlitz, and M. E. Fisher,

Renormalization-Group Analysis of Bicritical and Tetracritical Points Phys. Rev. Lett. **33**, 813 (1974); J. M. Kosterlitz, D. R. Nelson, and M. E. Fisher, Bicritical and tetracritical points in anisotropic antiferromagnetic systems, Phys. Rev. B **13**, 412 (1976).

[31] A. Pelissetto and E. Vicari, Critical phenomena and renormalization group theory, Phys. Rep. **368**, 549 (2002).

[32] P. Calabrese, A. Pelissetto, and E. Vicari, Multicritical behavior of $O(n_1) \oplus O(n_2)$-symmetric systems, Phys. Rev. B **67**, 054505 (2003).

[33] A. M. Ferrenberg, J. Xu, and D. P. Landau, Pushing the limits of Monte Carlo simulations for the three-dimensional Ising model, Phys. Rev. E **97**, 043301 (2018).

[34] M. Campostrini, M. Hasenbusch, A. Pelissetto, and E. Vicari, Theoretical estimates of the critical exponents of the superfluid transition in ^{4}He by lattice methods, Phys. Rev. B **74**, 144506 (2006).

[35] M. Hasenbusch and E. Vicari, Anisotropic perturbations in 3D O(N) vector models, Phys. Rev. B **84**, 125136 (2011).

[36] P. Calabrese, P. Parruccini, A. Pelissetto, and E. Vicari, Critical behavior of $O(2) \otimes O(N)$-symmetric models, Phys. Rev. B **70**, 174439 (2004).

[37] C Borgs and F. Nill, The Phase Diagram of the Abelian Lattice Higgs Model. A Review of Rigorous Results, J. Stat. Phys. **47**, 877 (1987).

[38] F. J. Wegner, *The Critical State, General Aspects*, in Phase Transitions and Critical Phenomena, ed. by C. Domb and M. S. Green, (Academic Press, NY, 1976).

[39] R. Guida and J. Zinn-Justin, Critical exponents of the N-vector model, J. Phys. A **31**, 8103 (1998).

[40] M. V. Kompaniets and E. Panzer, Minimally subtracted six-loop renormalization of ϕ^4-symmetric theory and critical exponents, Phys. Rev. D **96**, 036016 (2017).

[41] M. Hasenbusch, Monte Carlo study of an improved clock model in three dimensions, Phys. Rev. B **100**, 224517 (2019).

[42] S. M. Chester, W. Landry, J. Liu, D. Poland, D. Simmons-Duffin, N. Su, and A. Vichi, Carving out OPE space and precise O(2) model critical exponents, J. High Energy Phys. **06**, 142 (2020).

[43] J. Carmona, A. Pelissetto, and E. Vicari, The N-component Ginzburg-Landau Hamiltonian with cubic symmetry: a six-loop study, Phys. Rev. B **61**, 15136 (2000).

[44] N. Metropolis, A. W. Rosenbluth, M. N. Rosenbluth, A. H. Teller, and E. Teller, Equation of state calculations by fast computing machines, J. Chem. Phys. **21**, 1087 (1953).